



HAL
open science

Liquid chromatography-mass spectrometry based metabolomics investigation of different tissues of *Mytilus galloprovincialis*

Lea James, Elena Gomez, Gaëlle Ramirez, Thibaut Dumas, Frédérique Courant

► **To cite this version:**

Lea James, Elena Gomez, Gaëlle Ramirez, Thibaut Dumas, Frédérique Courant. Liquid chromatography-mass spectrometry based metabolomics investigation of different tissues of *Mytilus galloprovincialis*. *Comparative Biochemistry and Physiology - Part D: Genomics and Proteomics*, 2023, 45, pp.101051. 10.1016/j.cbd.2022.101051 . hal-03930806

HAL Id: hal-03930806

<https://hal.science/hal-03930806>

Submitted on 22 May 2024

HAL is a multi-disciplinary open access archive for the deposit and dissemination of scientific research documents, whether they are published or not. The documents may come from teaching and research institutions in France or abroad, or from public or private research centers.

L'archive ouverte pluridisciplinaire **HAL**, est destinée au dépôt et à la diffusion de documents scientifiques de niveau recherche, publiés ou non, émanant des établissements d'enseignement et de recherche français ou étrangers, des laboratoires publics ou privés.

1 Liquid chromatography-mass spectrometry based metabolomics
2 investigation of different tissues of *Mytilus galloprovincialis*

3 Lea James, Elena Gomez, Gaelle Ramirez, Thibaut Dumas and Frédérique Courant *

4 HydroSciences Montpellier, University of Montpellier, IRD, CNRS, Montpellier, France

5
6 HydroSciences Montpellier, 15 avenue Charles Flahault, 34090 Montpellier

7

8

9

10 * Corresponding author : email: frederique.courant@umontpellier.fr; tel: +0033411759414

11

12

13 **Acknowledgements & funding**

14 This research was funded by SANOFI France and the French Agence Nationale de la Recherche (IMAP ANR-
15 16-CE34-0006-01). The authors thank the Platform Of Non-Target Environmental Metabolomics (PONTEM)
16 of the Montpellier Alliance for Metabolomics and Metabolism Analysis (MAMMA) consortium facilities.

17

18

19 **Abstract**

20 The Mediterranean mussel (*Mytilus galloprovincialis*) is widely used in monitoring programs and in
21 ecotoxicological studies to examine the biological effects of physicochemical parameter changes and the impact
22 of chemical pollutants. Metabolomics has recently demonstrated high potential to gain further insight into the
23 molecular effects of chemical exposure and the success of its application is dependent on the extent of prior
24 metabolomics knowledge available on the target organism. Therefore, the purpose of this study was the
25 investigation of the metabolites of five different functional tissues of male and female Mediterranean mussels
26 (digestive gland, foot, gill and gonad tissues and in the remaining soft tissues) accessible to the analysis using
27 the most common sample preparation recommended for tissue analysis (i.e. Bligh & Dyer). Metabolic
28 fingerprints were acquired via liquid chromatography high-resolution mass spectrometry and the identification
29 was based on an internal database developed in the laboratory. It led to the identification of 110 metabolites,
30 among which amino acids, carboxylic acids, purine and pyrimidine metabolites were often the most abundant.
31 The metabolic contents of the five tissues quantitatively and qualitatively differed, with a clear distinction
32 between male and female contents observed in the gonads and digestive glands. These results underline the
33 importance of selecting the most suitable tissue and sex to study the impact of contamination on metabolism
34 and the need for further research to deeper characterize the metabolome of this organism.

35 **Keywords:** metabolomics, bivalve, gonad, foot, digestive gland, gill, soft tissue

36

37

1. Introduction

40 Bivalve molluscs—a major taxon in marine waters—include the Mediterranean mussel (*Mytilus*
41 *galloprovincialis*). The distribution range of this species extends from southwestern Britain to the Mediterranean
42 Sea. This mollusc is considered to be a crucial ecosystem engineer since it is responsible for enhancing the
43 presence of small invertebrates by increasing the habitat complexity and improving the environmental
44 conditions for coastal communities (Arribas et al., 2014). Mussels filter large volumes of water and can
45 bioaccumulate pollutants, thereby facilitating monitoring of their exposure to a variety of chemical contaminants
46 (Moreno-González et al., 2016; Faggio et al., 2018; López-García et al., 2019). Moreover, these organisms are
47 particularly interesting for monitoring programs and laboratory ecotoxicological studies due to their wide
48 geographical distribution, ability to tolerate different environmental conditions and suitability for *in situ* cage
49 experiments. Mussels actively respond to environmental changes via dynamic modifications in their physiology,
50 gene expression and metabolism (Connor & Gracey, 2011, 2012; Gracey & Connor, 2016; Yang et al., 2019;
51 Keskinbalta & Çelik, 2020). The ability of these organisms to rapidly react to changes in their surrounding
52 environment provides a basis for molecular profiling geared towards identifying specific transcriptomic,
53 proteomic or metabolomic profiles in response to different stresses.

54 Although the application of omics techniques in environmental science studies is recent, information can be
55 provided by these approaches to allow the assessment of molecular effects of environmental stressors on aquatic
56 organisms (Campillo et al., 2019; Lockwood et al., 2015; Tomanek & Zuzow, 2010). One of the most recent
57 omics approaches, i.e. metabolomics, concerns the metabolic profile of a cell or tissue or entire organism.
58 Investigated metabolites are generally of low molecular weight (50-1,500 Da) and occur in many essential
59 biological pathways. Their levels vary according to the physiological, developmental or pathological status of
60 cells, tissues, organs or whole organisms (Courant et al., 2014; Lin et al., 2006; Zhang et al., 2021). Two
61 analytical methods for metabolic fingerprinting are commonly used: nuclear magnetic resonance (NMR) and
62 mass spectrometry (MS) combined with component separation methods such as liquid chromatography (LC-
63 MS) and gas chromatography (GC-MS). Many ecotoxicology studies involving metabolomics have been
64 successfully carried out to unravel the effects of environmental stressors on mussels (Bonnefille et al., 2018;
65 Campillo et al., 2019; Cappello et al., 2015, 2017, 2020; Dumas et al., 2022; Ramirez et al., 2022).

66 However, although mussels are a key species for ecotoxicological studies, information on their metabolome is
67 still fragmentary. The choice of the tissue to be studied is important in ecotoxicological studies. Indeed, different
68 stressor exposure signatures may be observed depending on the investigated tissue (Jordan et al., 2012). Insight
69 into the metabolome of the different *M. galloprovincialis* tissues is therefore essential. Two studies already
70 reported knowledge on mussel metabolome for the purpose of species discrimination (Rochfort et al., 2013;
71 Utermann et al., 2018). The latter identified 76 major compounds dominated by pigments, alkaloids and
72 polyketides in whole tissue extracts. As the digestive gland and gills are the tissues focused on most commonly
73 in ecotoxicological studies, some metabolites have already been reported in these tissues following
74 environmental contaminant exposure (Song et al., 2016; Dumas et al., 2020a; Dumas et al., 2022). Gonads have
75 also been investigated to determine sex-specific differences in the mussel metabolome for the purpose of
76 reproductive physiology studies (Cubero-Leon et al., 2012) or to highlight hormonal differences (Martínez-Pita
77 et al., 2012). One NMR-based study provided an overview of concentrations of the main metabolites of three
78 functional tissues (digestive gland, gills and posterior adductor muscle) (Cappello et al., 2018). A total of 44
79 metabolites were thereby reported, with 27 being common to all three tissues, at 0.1–100 mM concentration.
80 The purpose of this study was to give information on male and female mussel metabolome and particularly on
81 mussel metabolites that can be accessible to the analysis using the most common sample preparation
82 recommended for tissue analysis (i.e. Bligh & Dyer) (Vuckovic, 2020) and Liquid Chromatography High
83 Resolution Mass Spectrometry (LC-HRMS). Mass spectrometry (MS) is more sensitive than NMR and may
84 therefore offer new opportunities for the detection of minor yet important compounds. This study was also
85 designed to estimate concentrations of the main metabolites of four different functional tissues of the
86 Mediterranean mussel (*M. galloprovincialis*), namely digestive gland (DG), foot (F), gill (G) and gonad (Go)
87 tissues and in the remaining soft tissues (S) which include mantle, muscles and palpes.

88

89

90

91

92 **2. Material and methods**

93 **2.1 Chemicals**

94 Ultrapure water was generated by a Simplicity UV system from Millipore (Bedford, MA, USA) with a specific
95 resistance of 18.2 MΩ.cm at 25°C. Pesticide analytical-grade solvents (methanol, dichloromethane and ethanol)
96 and LC/MS grade solvents (water, acetonitrile, formic acid 99%) were obtained from Carlo Erba (Val de Reuil,
97 France). Analytical pure standards were purchased from the four following suppliers: Sigma-Aldrich (now part
98 of Merck), Santa Cruz Biotechnology, Toronto Research Chemicals and LGC Standards. All chemicals used in
99 this study were analytical grade (> 95% purity).

100

101 **2.2 Animals**

102 *Mytilus galloprovincialis* mussels were obtained from a Mediterranean shellfish farm (Bouzigues, France) in
103 February 2017. Twenty mussels were collected and uniformly selected according to their shell size (6-8 cm).
104 They were depurated for 7 seven days in filtered seawater (provided by IFREMER, Palavas, France; filter GF/F
105 Ø 100 µm) and dissected. Sex determination was done by microscopy and 3 mature females and 3 males were
106 selected. Mussels were dissected on ice and five tissues were collected (digestive gland, foot, gill, gonad and
107 soft tissues). The samples were directly frozen and stored at -80°C prior to analysis.

108

109 **2.3 Tissue sample preparation**

110 This study was performed on 5 different tissues with 3 replicates for male and 3 for female mussels (n = 30).
111 Mussel tissues were freeze-dried and ground into a fine powder. The tissue sample preparation protocol was
112 previously described by Bonnefille et al. (2018). A biphasic methanol/dichloromethane/water (16/16/13; v/v/v)
113 solvent system was used. Briefly, 30 mg of each tissue sample (± 0.40 mg) were first homogenised and extracted
114 in a glass tube with 240 µL of methanol and 75 µL of water and vortexed for 1 min. In a second step, 240 µL
115 of dichloromethane and 120 µL of water were added and again vortexed. The samples were left at 4°C for 15
116 min and then vortexed and centrifuged at 2,000× g for 15 min at 4°C. 50 µL volumes of the supernatant (polar
117 phase) were collected and evaporated to dryness under a nitrogen stream and finally re-suspended in 200 µL of
118 water/acetonitrile (ACN) (95/5; v/v). The extracts were subsequently filtered directly into an analysis vial using
119 a 0.20 µm PTFE syringe filter (Minisart SRP 4, Sartorius). Five quality control (QC) samples corresponding to
120 each tissue were prepared by pooling 40 µL of each sample extract included in the experiment.

121

122 **2.4 LC-HRMS analysis**

123 The injections were randomly performed on a Vanquish HPLC (Thermo Fisher Scientific, Bremen, Germany)
124 coupled to a Q Exactive Orbitrap high resolution mass spectrometer (Thermo Fisher Scientific, Bremen,
125 Germany) equipped with a heated electrospray ionization source (HESI). A reversed phase
126 pentafluorophenylpropyl (PFPP) analytical column (100 × 2.1 mm; 3 μm particle size; Sigma Aldrich, PA,
127 Bellefonte, USA) was used for LC separation. 10 μL volumes of each sample were loaded onto the column with
128 full loop injection. The mobile phases were two mixtures of water/ACN (99/1; v/v) (phase A) or ACN/water
129 (99/1; v/v) (phase B), both modified with 0.1% formic acid. The flow rate was 250 μL/min and the following
130 gradient was applied (A/B): 95/5 from 0 to 3 min, 60/40 at 8 min, 50/50 at 9 min, 30/70 at 13 min and 5/95 from
131 15 to 18 min. From 18 to 21 min, the system was left to return to the starting conditions followed by a re-
132 equilibration period (95/5) of 7 min (total run time, 28 min).

133 The Q Exactive HRMS was tuned to a mass resolution of 35,000 (FWHM, m/z 200), with a mass spectrum
134 range of 50–750 m/z. Data were acquired simultaneously in both positive (ESI⁺) and negative (ESI⁻) ionization
135 modes with the following settings: 3.35 |kV| spray voltage, 55 sheath gas flow rate, 10 aux gas flow rate, 50 S-
136 Lens RF level, 300°C capillary temperature and 250°C heater temperature. Data independent acquisition (DIA)
137 was also applied on the QC_{tissue} samples with a high energy collision dissociation (HCD) cell set at 20 eV, with
138 a mass resolution of 17,500.

139

140 **2.5 Quality control and semi-quantification**

141 The QC samples were injected at the beginning, end and during the sequence to assess the analytical
142 repeatability of the acquisitions. In order to estimate the concentrations of the identified metabolites in mussel
143 tissues (ND: not detected; +/-: <0.1 mg/kg; +:0.1-1 mg/kg; ++:1-10 mg/kg; +++:10-100 mg/kg; ++++:>100
144 mg/kg), calibration curves were plotted by injecting increasing quantities of the pure target analytes from 0.015
145 to 15 ng injected on-column (corresponding to 0.01 to 10 mg/kg dw when considering a 30 mg sample size).

146

147 **2.6 Data processing and statistical analysis**

148 **2.6.1 Data processing**

149 Raw data were converted to .mzXML files with MSConvert freeware (ProteoWizard 3.0, Chambers et al., 2012).
150 Data were then processed using the XCMS package (Smith et al., 2006) in the R environment. Two treatments
151 were performed: all tissues together (n=30) and each tissue separately (n=6 for each tissue, n=3 per sex).
152 Optimized XCMS parameters were used: 0.002 m/z interval for peak picking, signal-to-noise ratio threshold of
153 10, the group bandwidth of 15, and 0.5 minimum fraction. XCMS returned results as a peak table containing
154 variable identity (i.e. m/z and retention time) and feature abundances (i.e. peak area). One file per tissue was
155 generated and one file containing the peak integrations in all tissues. Each extracted ion chromatogram (EIC)
156 was visually assessed to verify that each integrated signal corresponded to a Gaussian chromatographic peak.
157 All features corresponding to baseline drift or background noise were discarded from the dataset.

158

159 **2.6.2 Multivariate statistical analysis**

160 Principal component analysis (PCA) was performed on the table containing all the tissues results (SIMCA
161 13.0.3., Umetrics, Sweden) in order to reduce the dataset complexity and highlight mussel tissue- and sex-
162 specific metabolic differences. Datasets were log transformed and Pareto scaled prior to analysis.

163

164 **2.7 Metabolite identification**

165 Annotation was performed using an in-house database. This database consisted of 272 metabolites and their
166 characteristics (chemical formula, log P, retention time Rt with the same chromatographic column, positive and
167 negative adducts). Therefore, all annotations performed were of level 1 according to Sumner et al., (2007). Level
168 1 corresponds to annotation confirmed by injection of the analytical standard on the same analytical platform
169 under the same conditions (validation based on both accurate mass and retention time). Moreover, standard
170 addition was made in the matrix to confirm the retention time. Identified metabolites were assigned to subclasses
171 and direct parents according to HMDB. For identified metabolites, integrations were performed again manually
172 with Thermo FreeStyle software (Thermo Fisher Scientific, USA).

173

174 **2.8 Molecular network**

175 Using all MS/MS data (converted in mgf format with MZmine software) obtained for the five tissues, a
176 molecular network was created using the Global Natural Products Social Molecular Networking (GNPS) online

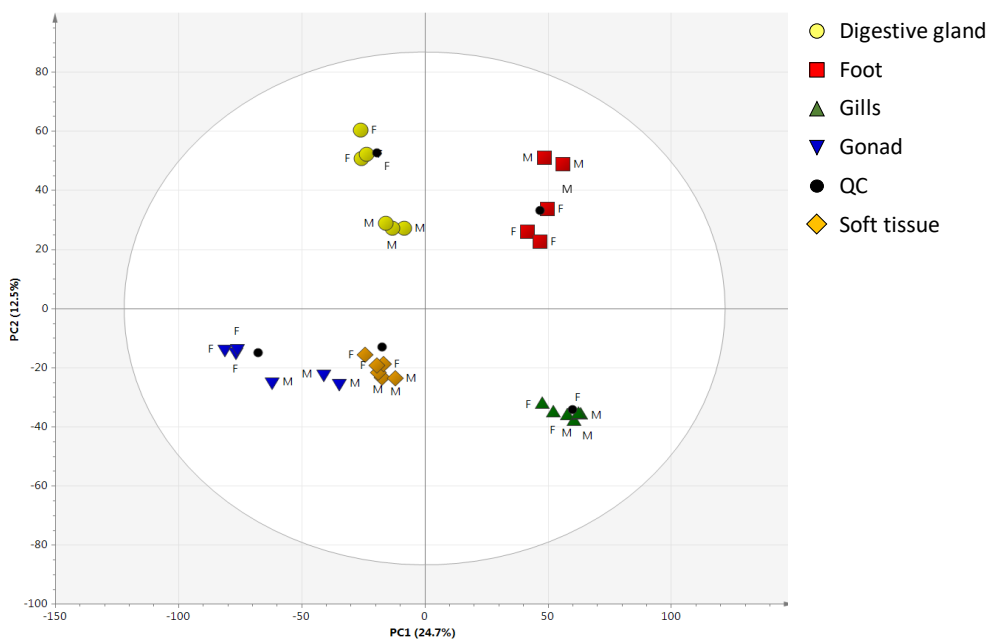
177 workflow (<http://gnps.ucsd.edu>). With MS-Cluster, the data were clustered with a parent mass tolerance of 0.002
178 Da and a MS/MS fragment ion tolerance of 0.002 Da. A network was then created where the edges were filtered
179 to have a cosine score > 0.6 with more than four matched fragment ions. Molecular networks were visualized
180 using Cytoscape 3.6.0. (NRNB & NIGMS, USA).

181

182 **3. Results**

183 LC-HRMS analyses of the 5 male and female mussel tissues were carried out in both negative and positive
184 electrospray ionization modes (ESI- & ESI+). The metabolic fingerprints provided 10,625 signals detected in
185 ESI- and 8,878 signals in ESI+. The analytical repeatability was acceptable, as demonstrated on the PCA score
186 plots in both ESI+ (Fig. 1) and ESI- (Supplementary Fig. 1), where the QC_{tissues} samples (n=3 per tissue) were
187 plotted together and along with their respective tissue samples.

188 Distinct clusters were observed between the 5 tissues (Fig. 1). According to the first principal component (PC1),
189 and the second component (PC2), there was a clear separation between the metabolome of the 5 tissues.
190 Moreover, a clear separation between male and female samples was noted in some tissues. Sexual metabolic
191 differentiation in gonad tissues was visible according to PC1, whereas this differentiation was observable
192 according to PC2 for digestive gland and foot tissues. Similar patterns were noted in ESI- (Supplementary Fig.
193 1).



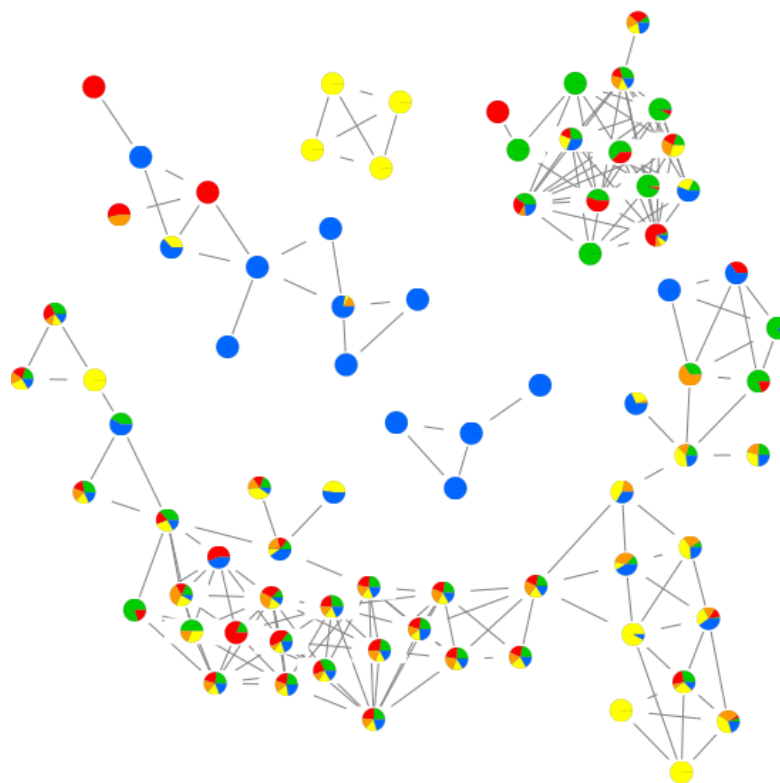
194

195 **Fig. 1** PCA score plot of ESI + metabolic fingerprints from digestive gland (yellow circle), foot (red square),
 196 gill (green triangle), gonad (inverted blue triangle) and soft (orange diamond) mussel tissues showing a clear
 197 separation between these tissues. In black (circle), the QC_{tissue} are shown. (Note that interpretation of the
 198 references to colour in this figure legend are provided in the web version of this article)

199

200 A molecular network was obtained, showing clusters of compounds with spectral similarities (Supplementary
 201 Fig. 2). Interestingly, there were clusters shared between all tissues, thus demonstrating the absence of tissue
 202 specificity for these metabolites, while other clusters appeared to be specific to one tissue (Fig. 2).

203



204

205 **Fig. 2** Small selection of clusters highlighted by GNPS analysis based on MS/MS fragmentation spectra
 206 obtained from the different Mediterranean mussel tissues. The color code is as follows: digestive gland (yellow),
 207 foot (red), gill (green), gonad (blue) and soft (orange) tissues. The relative intensity of the metabolite in each
 208 tissue is represented as a pie chart on each node

209

210 Based on our in-house database, 110 metabolites were identified in the 5 tissues (87 in gill, 102 in gonad, 102
 211 in digestive gland, 90 in foot and 105 in soft tissues). A list of metabolites identified in the different tissues with
 212 a distinction between male and female samples is given in Table 1, along with their characteristics in positive
 213 and negative ESI and their abundances. Some metabolites were found to be present in large quantities in all
 214 tissues compared to others, such as betaine, proline betaine and succinic acid (> 100 mg/kg dw). These
 215 metabolites were present at 100- and 50-fold higher concentrations than most of the other identified compounds.
 216 Other compounds were also noted at high concentrations specifically in one or more tissues, such as
 217 glycerophosphorylcholine, adenosine related compounds or deoxyribose. Three amino acids (glycine, arginine
 218 and L-aspartic acid) were also abundant, with concentrations of >100 mg/kg dw. A large proportion of the
 219 identified metabolites belonged to the amino acid subclass, such as serine, threonine and tyrosine metabolites.
 220 Purine and pyrimidine subclasses were also detected with many intermediates, including their respective

221 nucleotides and nucleosides, which were identified. Differences in abundance of specific metabolites were noted
222 when comparing male or female samples (Table 1, e.g. 2-methylglutaric acid in gonad tissues or adenosine in
223 foot, digestive gland and soft tissues). Indeed, as depicted in Fig. 1, gonad and digestive gland tissues showed
224 differentiation between male and female tissues.

225

226

227 *Table 1: Estimation of the concentrations of metabolites (mg/kg dw, ppm) observed in gill, gonad, digestive gland, foot and soft tissues in female and male mussels (mean*
 228 *abundances for each sex; ND: not detected; +/-: <0.1 ppm; +:0.1-1 ppm; ++:1-10 ppm; +++:10-100 ppm; +++++:>100 ppm)*

Sub-class (HMDB)	Direct parent (HMDB)	Metabolite	Rt (min)	ESI +		ESI-		Abundances in tissues									
				Adduct	m/z	Adduct	m/z	Male gills	Female gills	Male Gonads	Female Gonads	Male digestive glands	Female digestive glands	Male feet	Female feet	Soft Male tissues	Soft Female tissues
Alcohols and polyols	Secondary alcohols	Pantothenic acid	2,94	[M+H] ⁺	220,1179	[M-H] ⁻	218,1034	+	+	++	++	+	+	+	+	++	++
Alkaloids and derivatives	Alkaloids and derivatives	Trigonelline	1,55	[M+H] ⁺	138,0550	[M+FA-H] ⁻	182,0459	ND	+	++	++	++	++	+/-	+/-	++	++
Alkyl-phenylketones	Alkyl-phenyl ketones	DL-kynurenine	9,17	[M+H] ⁺	209,0921			+	+	+	+	+	+	+/-	+/-	+	+
		N-Acetyl-5-methoxykynuramine (AMK)	11,33	[M+H] ⁺	237,1234			ND	ND	+	+	+	+	+	+	+	ND
Amines	2-arylethylamines	Histamine	5,34	[M+H] ⁺	112,0869			+/-	+/-	+/-	+/-	+/-	+/-	+/-	+/-	+/-	+/-
	Alanine and derivatives / Alpha amino	L-Alanine/Sarcosine	1,49	[M+H] ⁺	90,0550	[M-H] ⁻	88,0404	++	+++	+++	+++	+++	+++	+++	+++	+++	+++
		Betaine	1,41	[M+H] ⁺	118,0863	[M+FA-H] ⁻	162,0772	+++	+++	+++	+++	+++	+++	+++	+++	+++	+++
	Alpha amino acids	Glycine	1,37	[M+H] ⁺	76,0393	[M-H] ⁻	74,0248	+++	+++	+++	+++	+++	+++	+++	+++	+++	+++
		Pipecolic acid / pipecolinic acid	2,52	[M+H] ⁺	130,0863			+/-	+/-	+	+	+	+	+	+	+	+
	Alpha amino acids and derivatives	Pyroglutamic acid = 5-oxoproline	1,91	[M+H] ⁺	130,0499	[M-H] ⁻	128,0353	+	+	++	++	++	++	+/-	+/-	++	++
	Aspartic acid and derivatives	L-Aspartic acid	1,33	[M+H] ⁺	134,0448	[M-H] ⁻	132,0302	+++	+++	+++	+++	+++	+++	+++	+++	+++	+++
	Beta amino acids and derivatives	N-Acetyl-L-aspartic acid	1,65	[M+H] ⁺	176,0553	[M-H] ⁻	174,0408	+	+	+	+	+	+	+	+	ND	+
		(s)-b-aminoisobutyric acid	2,83	[M+H] ⁺	104,0706			+	+	++	+	+	+	+	+	+	+
	Beta amino acids and derivatives	beta-Alanine	2,28	[M+H] ⁺	90,0550			+	+	++	++	++	++	++	++	++	++
	Gamma amino acids and derivatives	Gamma-L-glutamyl-L-leucine	9,91	[M+H] ⁺	261,1445	[M-H] ⁻	259,1299	+	+	+	+	+	+	+	+	+	+
	Gamma amino acids and derivatives	gamma-Aminobutyric acid (GABA)	2,58	[M+H] ⁺	104,0706			+	+	+	+	+	+	++	++	+	+
	Glutamic acid and derivatives	L-Glutamic acid	1,47	[M+H] ⁺	148,0604	[M-H] ⁻	146,0459	+++	+++	+++	+++	+++	+++	+++	+++	+++	+++
		N-Acetyl-L-glutamic acid	1,92			[M-H] ⁻	188,0564	ND	ND	ND	+/-	+/-	+	ND	ND	+/-	ND
	Histidine and derivatives	L-Histidine	2,33	[M+H] ⁺	156,0768	[M-H] ⁻	154,0622	+	+	++	++	++	++	++	++	++	++
	Indolyl carboxylic acids and	L-Tryptophan	11,77	[M+H] ⁺	205,0972	[M-H] ⁻	203,0826	++	++	+++	+++	+++	+++	++	++	+++	+++
	Isoleucine and derivatives	L-Isoleucine	4,60	[M+H] ⁺	132,1019	[M-H] ⁻	130,0874	+	+	++	++	++	++	++	++	++	++
		N-Acetylisoleucine	9,72	[M+H] ⁺	174,1125	[M-H] ⁻	172,0979	ND	ND	+/-	+/-	+/-	+/-	ND	ND	+/-	+/-
Amino acids, peptides and analogues		L-Allothreonine	1,35	[M+H] ⁺	120,0655	[M-H] ⁻	118,0510	++	++	+++	+++	+++	+++	++	+++	+++	+++
		L-alpha-Aminobutyric acid/2-aminoisobutyric acid	2,30	[M+H] ⁺	104,0706			++	++	++	+	++	+	++	++	++	+
		L-Arginine	2,62	[M+H] ⁺	175,1190	[M-H] ⁻	173,1044	+++	+++	+++	+++	+++	+++	+++	+++	+++	+++
		L-Glutamine	1,35	[M+H] ⁺	147,0764	[M-H] ⁻	145,0619	+	++	+++	+++	+++	+++	++	++	+++	+++
	L-alpha amino acids	L-Homocysteic acid	1,13	[M+H] ⁺	184,0274			+	+	++	++	+	++	+	+	+	+
		L-Lysine	2,54	[M+H] ⁺	147,1128	[M-H] ⁻	145,0983	++	++	+++	+++	+++	++	++	++	+++	+++
		L-Ornithine	2,38	[M+H] ⁺	133,0972			+	+	++	++	++	++	++	++	++	++
		L-Threonine/L-Homoserine	1,43	[M+H] ⁺	120,0655	[M-H] ⁻	118,0510	ND	ND	++	+++	+++	++	++	++	++	++
		N6-Acetyl-L-lysine	2,01	[M+H] ⁺	189,1234	[M-H] ⁻	187,1088	+/-	+/-	+	+/-	+	+/-	+/-	ND	+/-	+/-
	Leucine and derivatives	L-Leucine	5,07	[M+H] ⁺	132,1019			++	++	++	++	++	++	++	++	++	++
	Methionine and derivatives	L-Methionine	2,70	[M+H] ⁺	150,0583			+	+	+	ND	++	++	++	++	++	++
	N-acyl-L-alpha amino acids	N-Acetyl-L-alanine	1,98	[M+H] ⁺	132,0655	[M-H] ⁻	130,0510	+	+	+	+	+	+	+	+/-	+	+
		N-Acetyl-L-threonine	1,67	[M+H] ⁺	162,0761	[M-H] ⁻	160,0615	++	++	+	+	++	++	++	++	++	++
	Oligopeptides	Ophthalmic acid	2,02	[M+H] ⁺	290,1347	[M-H] ⁻	288,1201	+/-	+/-	+	+/-	ND	ND	ND	ND	+	+
	Peptides	Oxidized glutathione	2,27	[M+2H] ⁺	307,0833	[M-H] ⁻	611,1447	++	++	++	++	++	++	++	++	++	++
	Phenylalanine and derivatives	L-Phenylalanine	8,25	[M+H] ⁺	166,0863	[M-H] ⁻	164,0717	++	++	+++	+++	+++	+++	+++	+++	+++	+++
		N-Acetyl-L-phenylalanine	11,06	[M+H] ⁺	208,0968	[M-H] ⁻	206,0823	ND	ND	+/-	+/-	+/-	+/-	ND	ND	+/-	+/-
		4-Hydroxyproline	1,33	[M+H] ⁺	132,0655	[M-H] ⁻	130,0510	+	+	++	++	++	++	+	+	++	++
	Proline and derivatives	L-Proline	1,51	[M+H] ⁺	116,0706			++	++	+++	+++	+++	+++	++	++	+++	+++
		Proline betaine	1,59	[M+H] ⁺	144,1019	[M+FA-H] ⁻	188,0928	+++	+++	+++	+++	+++	+++	+++	+++	+++	+++

Sub-class (HMDB)	Direct parent (HMDB)	Metabolite	Rt (min)	ESI +		ESI-		Abundances in tissues										
				Adduct	m/z	Adduct	m/z	Male gills	Female gills	Male Gonads	Female Gonads	Male digestive glands	Female digestive glands	Male feet	Female feet	Soft Male tissues	Soft Female tissues	
	Serine and derivatives	L-Serine	1,35	[M+H] ⁺	106,0499	[M-H] ⁻	104,0353	++	++	+++	+++	+++	++	++	++	++	+++	+++
		3,4-Dihydroxy-L-phenylalanine (L-Dopa)	2,81	[M+H] ⁺	198,0761	[M-H] ⁻	196,0615	ND	ND	ND	ND	ND	ND	++	++	ND	++	
	Tyrosine and derivatives	Gamma-glutamyltyrosine	7,65	[M+H] ⁺	311,1238			ND	ND	ND	+	+	+	ND	ND	ND	ND	
		L-Tyrosine	3,65	[M+H] ⁺	182,0812	[M-H] ⁻	180,0666	++	+++	++++	+++	++++	+++	+++	+++	+++	+++	+++
		N-Acetyl-L-tyrosine	8,44	[M+H] ⁺	224,0917	[M-H] ⁻	222,0772	ND	ND	+/-	+/-	+/-	+/-	ND	ND	+/-	+/-	
	Valine and derivatives	L-Valine	2,43	[M+H] ⁺	118,0863	[M-H] ⁻	116,0717	++	++	++	++	++	++	++	++	++	++	
		N-Acetylvaline	5,45	[M+H] ⁺	160,0968	[M-H] ⁻	158,0823	ND	ND	+	+	+/-	+	ND	ND	+/-	+/-	
	2(hydroxyphenyl)acetic acids	Homogentisic acid	4,48			[M-H] ⁻	167,0350	ND	ND	ND	ND	ND	ND	+/-	ND	ND	+/-	
	Benzoic acids	Phthalic acid	9,88	[M+H ₂ O+H] ⁺	149,0228	[M-H] ⁻	165,0193	+/-	+/-	+/-	+/-	+/-	+	+/-	+/-	+/-	+/-	
	dimethoxybenzenes	Homoveratric acid	11,58	[M+H] ⁺	197,0808	[M-H] ⁻	195,0663	ND	ND	+/-	+/-	ND	ND	ND	ND	+/-	+/-	
	Phenylacetamides	2-Phenylacetamide	9,30	[M+H] ⁺	136,0757			+/-	+/-	+/-	+/-	+/-	+/-	+/-	+/-	+/-	+/-	
	Benzoic acids and derivatives	Formylanthranilic acid	11,83	[M+H] ⁺	166,0499	[M-H] ⁻	164,0353	+/-	+/-	+	+/-	+/-	+	+/-	+/-	+	+	
	Acylaminosugars	N-Acetyl-D-glucosamine	1,30	[M+H] ⁺	222,0972	[M+Cl] ⁻	256,0593	+++	+++	++	++	+++	+++	++	++	++	++	
		N-Acetylmannosamine	1,32	[M+H ₂ O+H] ⁺	204,0861	[M+FA-H] ⁻	266,0881	+	+	+	+	++	++	+/-	ND	+	+	
	Sugar acids and derivatives	Gluconic acid	1,21			[M-H] ⁻	195,0510	ND	ND	+	+	++	++	+	+	+	+	
		Glyceric acid	1,32			[M-H] ⁻	105,0193	+	+	++	++	++	++	++	++	++	++	
	Carboxylic acids	Glyoxylic acid	1,44			[M-H] ⁻	72,9931	++	++	++	++	++	++	+++	++	++	++	
		Fumaric acid	2,17			[M-H] ⁻	115,0037	+	+	+	+	+	+	+	+	+	+	
		Glutaric acid	2,77			[M-H] ⁻	131,0350	+	+	+++	+++	++	++	+	+	++	++	
	Dicarboxylic acids and derivatives	Maleic acid	2,85			[M-H] ⁻	115,0037	+/-	+/-	+	+	+	+	+/-	+/-	+	+	
		Malonic acid	1,65			[M-H] ⁻	103,0037	+	+	++	++	+	++	+	+	++	++	
		Succinic acid	2,07	[M+2Na-H] ⁺	162,9978	[M-H] ⁻	117,0193	++++	++++	++++	++++	++++	++++	++++	++++	++++	++++	
	N-acetyl-2-arylethylamines	N-Acetylhistamine	3,26	[M+H] ⁺	154,0975			+/-	+/-	ND	ND	ND	ND	ND	ND	ND	ND	
	Tricarboxylic acids and derivatives	Citric acid	1,55			[M-H] ⁻	191,0197	+	+	+	+	+	+	++	++	++	++	
	Long chain fatty acids	Tetradecanedioic acid	14,43			[M-H] ⁻	257,1758	+	+	+	+	+	+	+	+	+	+	
	Medium chain fatty acids	Pimelic acid	9,18	[M+H ₂ O+H] ⁺	143,0697	[M-H] ⁻	159,0663	+	+/-	++	++	+	++	+/-	+/-	+	+	
	Methyl-branched fatty acids	2-Methylglutaric acid	4,80			[M-H] ⁻	145,0506	+	+	++	+++	++	++	+/-	+/-	++	++	
	Straight chain fatty acids	Succinic acid semialdehyde	9,64			[3M-H] ⁻	305,0878	ND	ND	+/-	+/-	ND	ND	ND	ND	+/-	+/-	
	Acyl carnitines	L-Acetylcarnitine	6,32	[M+H] ⁺	204,1230	[M+FA-H] ⁻	248,1140	+	+	+	+	+	++	++	++	++	++	
	Glycerophospholipids	Glycerophosphocholines	1,20	[M+H] ⁺	258,1101	[M+Cl] ⁻	292,0722	+++	+++	+++	++++	++++	++++	+++	+++	+++	+++	
	Beta hydroxy acids and derivatives	L-Malic acid	1,44			[M-H] ⁻	133,0142	+++	+++	+++	+++	+++	+++	+++	+++	+++	+++	
	Alpha-keto acids and derivatives	Pyruvic acid	1,58			[M-H] ⁻	87,0088	+	+	+	++	++	+	+	+	++	++	
	Medium chain keto acids and derivatives	Oxoadipic acid	1,92			[M-H] ⁻	159,0299	ND	ND	+	+	+/-	+/-	ND	ND	+/-	+	
	Short-chain keto acids and derivatives	3-Methyl-2-oxovaleric acid	8,35			[M-H] ⁻	129,0557	ND	ND	ND	ND	+	+	+	+	+	+	
	Methoxyphenols	Normetanephrine	5,38	[M+H ₂ O+H] ⁺	166,0857			ND	ND	+	+	ND	ND	ND	ND	+	+	
	Organic phosphoric acids and derivatives	Phosphoglycolic acid	1,00	[M+H] ⁺	156,9897			+	ND	++	++	++	++	+	ND	++	++	
	Pentoses	Deoxyribose	1,29			[M+FA-H] ⁻	179,0561	+++	++	+++	+++	+++	++++	+++	+++	+++	+++	
	Phenethylamines	Phenylethylamine	14,10	[M+H] ⁺	122,0964			+/-	+/-	+	+	+/-	+/-	+/-	+/-	+	+/-	
		Tyramine	8,50	[M+H] ⁺	138,0913			+/-	+/-	+/-	+	+	+/-	ND	ND	+/-	+/-	
	Phenols	1-hydroxy-2-unsubstituted p-octopamine	3,67	[M+H ₂ O+H] ⁺	136,0751			+	+	++	++	++	++	+	++	++	++	
	Phenylacetaldehydes	3,4-Dihydroxymandelaldehyde	5,10			[M-H] ⁻	167,0350	ND	ND	+	+	++	++	ND	ND	++	++	
		L-3-phenyllactic acid	10,88			[M-H] ⁻	165,0557	ND	ND	ND	+/-	+/-	+/-	+/-	ND	+/-	+/-	
	Phenylsulfates	Phenylsulfates	2,39			[M-H] ⁻	232,0285	+	+	+	ND	+	+	+	+	+	+	
	Purine 2'-deoxyribonucleosides	2'-Deoxyguanosine	2,48	[M+H] ⁺	268,1040	[M-H] ⁻	266,0895	+/-	ND	+	ND	+	+	ND	ND	+	ND	
		Adenosine	3,32	[M+H] ⁺	268,1040	[M+FA-H] ⁻	312,0950	++	++	++++	++++	++++	+++	+++	++	+++	++	
	Purine nucleosides	Guanosine	2,12	[M+H] ⁺	284,0989	[M-H] ⁻	282,0844	++	+	++	++	++	++	+	+	++	++	
		Inosine	1,92	[M+H] ⁺	269,0880	[M-H] ⁻	267,0735	++	++	++	++	+++	+++	++	++	++	++	
	Purine ribonucleoside diphosphates	Adenosine diphosphate (=ADP)	1,12	[M+H] ⁺	428,0367	[M-H] ⁻	426,0221	+++	+++	++++	++++	++++	++++	+++	+++	++++	++++	

Sub-class (HMDB)	Direct parent (HMDB)	Metabolite	Rt (min)	ESI +		ESI-		Abundances in tissues									
				Adduct	m/z	Adduct	m/z	Male gills	Female gills	Male Gonads	Female Gonads	Male digestive glands	Female digestive glands	Male feet	Female feet	Soft Male tissues	Soft Female tissues
	Purine ribonucleoside	Adenosine monophosphate (=5'AMP)/3'AMP	1,31	[M+H] ⁺	348,0704	[M-H] ⁻	346,0558	++	++	+++	+++	+++	+++	+++	+++	+++	+++
	6-aminopurines	Adenine	3,03	[M+H] ⁺	136,0618	[M-H] ⁻	134,0472	+	+	++	++	+	+	+	+	++	+
Purines and purines derivatives	Hypoxanthines	Hypoxanthine	1,91	[M+H] ⁺	137,0458	[M-H] ⁻	135,0312	+	+	+	+	+	++	+	+/-	+	+
	Purines and purine derivatives	Guanine	2,46	[M+H] ⁺	152,0567	[M-H] ⁻	150,0421	+	+	++	+	+	+	+	+	++	++
	Xanthines	Xanthine	1,90	[M+H] ⁺	153,0407	[M-H] ⁻	151,0261	+/-	ND	+/-	+/-	+/-	+/-	+	+/-	+	+
	Nicotinamides	Niacinamide (=nicotinamide)	2,62	[M+H] ⁺	123,0553	[M+FA-H] ⁻	167,0462	+	+	++	+	+	+	+	+	++	++
Pyridinecarboxylic acids and derivatives	Pyridine carboxylic acids	Nicotinic acid (vitamine B3)	2,02	[M+H] ⁺	124,0393	[M-H] ⁻	122,0248	++	++	++	++	++	++	+	+	++	++
	Cytidine	Cytidine	2,78	[M+H] ⁺	244,0928	[M+FA-H] ⁻	288,0837	+	+	++	+++	++	++	+	+	++	++
Pyrimidine nucleosides	Pyrimidine nucleosides	Uridine	1,91	[M+H] ⁺	245,0768	[M+FA-H] ⁻	289,0677	++	++	++	++	++	+++	++	+	++	++
	Deoxycytidine	Deoxycytidine	3,23	[M+H] ⁺	228,0979	[M+FA-H] ⁻	272,0888	ND	ND	+	+	+	+	ND	ND	+	+
	Deoxyuridine	Deoxyuridine	1,96	[M+H] ⁺	243,0975	[M+FA-H] ⁻	273,0728	ND	ND	+/-	ND	ND	+/-	ND	ND	+/-	ND
	Thymidine	Thymidine	2,71	[M+H] ⁺	243,0975	[M+FA-H] ⁻	287,0885	ND	ND	+	ND	+	+	ND	ND	+	ND
Pyrimidines and pyrimidine derivatives	Hydroxypyrimidines	Thymine	1,60	[M+H] ⁺	127,0502	[M-H] ⁻	125,0357	++	++	+++	+++	++	++	+	+/-	+++	++
	Pyrimidones	Cytosine	2,55	[M+H] ⁺	112,0505	[M-H] ⁻	111,0200	+/-	+/-	+	+	+	+	ND	ND	+	+
	Uracil	Uracil	1,64	[M+H] ⁺	112,0505	[M-H] ⁻	111,0200	+	+	+	+	+	++	++	+	++	++
	2-Pyrrolidinone	2-Pyrrolidinone	2,03	[M+H] ⁺	86,0600	[M-H] ⁻	85,0454	++	++	++	++	+	+	++	++	++	+
Quaternary ammonium salts	Carnitines	L-Carnitine	2,80	[M+H] ⁺	162,1125	[M+FA-H] ⁻	206,1034	++	++	++	++	++	++	++	++	++	++
Quinolines and derivatives	Quinoline carboxylic acids	Kynurenic acid	10,88	[M+H] ⁺	190,0499	[M-H] ⁻	188,0353	ND	ND	+/-	+/-	+/-	+/-	ND	ND	+/-	+/-
Sulfinic acids	Sulfinic acids	Hypotaourine	1,22	[M+H] ⁺	110,0270	[M-H] ⁻	108,0125	++	++	ND	ND	+++	+++	+++	+++	++	++
Tryptamines and derivatives	Serotonins	Serotonin	10,78	[M+H] ⁺	177,1022	[M-H] ⁻	175,0876	+	++	+/-	+/-	+	+/-	++	++	+	+

4. Discussion

The purpose of this study was to give information on mussel metabolome and particularly on mussel metabolites that can be accessible to the analysis using the most common sample preparation recommended for tissue analysis (i.e. Bligh & Dyer). Acquisitions were performed with LC-HRMS and identifications were conducted with an internal database (suspect screening approach).

Main metabolites belong to amino acids, carboxylic acids and purine nucleosides sub-classes

One hundred and ten metabolites were identified. The most detected subclasses were amino acids, carboxylic acids and purine and pyrimidine metabolites. Three amino acids were present in large quantities in tissues (glycine, L-aspartic acid and arginine) which had already been found in significant quantities in digestive glands according to Cappello et al. (2018). Betaine and proline betaine markedly prevailed over the other metabolites in all 5 tissues. Indeed, osmolytes such as betaine as well as some free amino acids, are the most abundant metabolites in *Mytilus galloprovincialis* according to Rochfort et al. (2013) and Cappello et al. (2018). These osmolytes are natural compounds that actively accumulate to allow the cells to adapt quickly to variations, such as osmotic stress (Pulliainen et al., 2010). Glycerophosphorylcholine has also been detected in large quantities, and is noteworthy for its osmolytic nature but also for its involvement, as a choline derivative, in cellular health (Kidd, 2005). Cappello et al. (2018) reported significant concentrations of glutamic acid, as also confirmed by our results. Indeed, glutamic acid is a precursor of glutamine, which is itself a constituent of oligopeptides such as glutathione. This amino acid has a major role in the protection mechanism against oxidative stress. Intermediates involved in energy metabolism (ADP, succinic acid, aspartic acid) are also widespread in the different tissues along with purine nucleosides.

Sensitivity of mass spectrometry is an asset

Metabolomics data on *M. galloprovincialis* are fragmentary, although some studies have already been conducted to gain knowledge on circulating metabolites in mussels (Belivermiş et al., 2020; Cappello et al., 2018; Rochfort et al., 2013; Utermann et al., 2018). Most of the metabolites detected by Cappello

257 et al. (2018) were identified in this study, along with those identified by Rochfort et al. (2013) and
258 Belivermiş et al. (2020). Some other metabolites were specifically detected in this study, e.g. cytosine
259 and DL-kynurenine. Cytosine is a pyrimidine base, found in DNA as a nucleotide. The kynurenine
260 pathway is in Human connected to the immune system and the *de novo* synthesis of nicotinamide
261 adenine dinucleotide (NAD⁺), which plays a critical role in many enzymatic redox reactions and in
262 mitochondrial energy production (Castro-Portuguez & Sutphin, 2020). Immune system and energy
263 metabolism disruption along with a down modulation of DL-kynurenine were observed in mussels
264 exposed to a WWTP extract (Dumas et al., 2020b). The detection of such compounds was probably due
265 to the higher detection sensitivity of mass spectrometry over NMR. Conversely, several compounds,
266 such as glucose, glycogen, taurine and homarine which were found in high concentrations in the studies
267 of Belivermiş et al. (2020), Cappello et al. (2018) and Rochfort et al. (2013), were not screened and
268 reported in Table 1 since data on these particular compounds were not available in our internal database.

269

270 ***Specificity between tissues was observed***

271 A certain specificity between tissues was observed as already described by Cappello et al. (2018).
272 However, we cannot ensure that concentrations in tissues are not impaired by lower recoveries or matrix
273 effects for certain specific metabolites. Some identified metabolites (Table 1) were specifically detected
274 in one or two tissues. For example, L-dopa was detected in feet and soft tissues. This result was not
275 surprising given the fact that L-dopa is a component of adhesive proteins that occur in high proportions
276 in byssus tissues (Bandara et al., 2013) formed in a gland located in the foot. Serotonin, which was
277 detected only in gills by Cappello et al. (2018) was detected predominantly in gills (and foot) in this
278 study. Serotonin having several physiological roles, e.g. contraction or relaxation of the adductor
279 muscles responsible for valves opening or closing, involvement in reproductive functions and ciliary
280 activity, its detection in all the investigated tissues of this study was then not surprising. Many other
281 detected metabolites seemed to be tissue-specific according to the molecular network results, where
282 clusters specific to one tissue were observed (Fig. 2, Supplementary Fig. 2). Metabolic similarities
283 between gonad and soft tissues were observed that may be due to the fact that mussels were collected
284 in their reproductive period, during which the mantles of mussels (i.e. the main soft tissue component)

285 fill with gamete-containing follicles (Anantharaman & Craft. 2012). Since the metabolic content is to
286 some extent different between tissues, these metabolic differences should be taken into consideration
287 when studying stressor effects in this species. For a large number of metabolites, significantly higher
288 concentrations were observed in three tissues (digestive gland, gonad and soft tissues). In order to be as
289 representative as possible of the effects of stress in ecotoxicological studies (when no prior hypotheses
290 enable target tissue selection), a maximum number of metabolites should be detected, which is easier
291 when there are high tissue concentrations. Studying these three tissues will preferentially facilitate the
292 detection of many metabolites. In particular, soft tissue is the tissue with the greatest mass available for
293 analysis. However, it is less specific to a biological function due to its complex composition involving
294 many organs (mantle, various muscles, heart and mouth) and the results may hence be hard to interpret.
295 The digestive gland—where high concentrations are also observed and from which it is possible to
296 obtain a reasonable sample size for analysis (unlike gonad tissues) is thus a very interesting target tissue
297 in ecotoxicological studies. In particular, the digestive gland is a tissue commonly used to measure
298 biological parameters (Bonfille et al., 2018; Campillo et al., 2019; Serra-Compte et al., 2019) because
299 it has a higher absorption and bioaccumulation capacity than other tissues (Faggio et al., 2018).

300

301 *Sexual dimorphism was confirmed*

302 The sexual metabolic differentiation observed in gonads (Fig. 1) has already been described by Cubero-
303 Leon et al. (2012) and Martínez-Pita et al. (2012). Both highlighted quantitative differences in fatty acid
304 (Martínez-Pita et al., 2012) and eicosanoid (Cubero-Leon et al., 2012) compositions. These differences
305 were explained in terms of the specific needs of males and females during gametogenesis and/or of the
306 differences in sperm and oocyte composition. The sexual metabolic differentiation observed in gonad
307 and digestive gland tissue samples may explain the different responses between males and females
308 observed following contaminant exposure (Dumas et al., 2020b; Liu et al., 2014; Zhang et al., 2017;
309 Ramirez et al., 2022). Notably, a different response of male and female mussels to venlafaxine exposure
310 was demonstrated by our group (Ramirez et al., 2022) in digestive gland tissues. Male and female
311 mussels showed several sex-specific impacted metabolites as well as differences in metabolite
312 modulation, such as an increase (glycine) or decrease (L-tyrosine) in only one of the two sexes, thereby

313 implying that they have different protective mechanisms in response to stress, especially with regard to
314 energy metabolism. These metabolites were quantified at different concentrations for the two sexes in
315 our study. The sexual metabolic differentiation in non-exposed organisms—although we cannot
316 confirm that the mussels were not exposed to a variety of contaminants in the Thau lagoon where they
317 had been reared and that the 1-week depuration period in the lab was sufficient to recover a baseline
318 metabolome—due to differences in their physiological needs may explain the sex-specific responses
319 observed after stress exposure. Further studies on the metabolome of digestive glands and gonads in a
320 large number of samples along with ecotoxicology studies on both sexes would be interesting to
321 precisely explain these metabolic differences and thus enhance the overall understanding of sex-specific
322 responses to pollutants.

323

324 **5. Conclusion**

325 One hundred and ten metabolites belonging to different metabolic pathways were identified via liquid
326 chromatography high resolution mass spectrometry in five tissues collected from *Mytilus*
327 *galloprovincialis*. All tissues were dominated by the osmolytes betaine and proline betaine, as well as
328 intermediates that have a role in energy metabolism (ADP, succinic acid and aspartic acid). This study
329 revealed marked differences between the 5 studied tissues. The choice of appropriate tissue according
330 to the target objectives of ecotoxicological studies is thus important. Digestive gland, gonad and soft
331 tissues showed higher levels of all metabolites. Sex-specific differences between the digestive gland
332 and gonad tissues in relation to the specific needs and metabolisms of males and females were also
333 observed. Overall, the results of this study will help enhance mussel tissue characterization, while also
334 being useful for future metabolomics studies focused on the effects of environmental contaminants on
335 *Mytilus* spp.

336

337 **References**

338 Anantharaman, S., & Craft, J. A. (2012). Annual Variation in the Levels of Transcripts of Sex-
339 Specific Genes in the Mantle of the Common Mussel. *Mytilus edulis*. PLoS ONE, 7(11), e50861.
340 <https://doi.org/10.1371/journal.pone.0050861>

341 Arribas, L. P., Donnarumma, L., Palomo, M. G., & Scrosati, R. A. (2014). Intertidal mussels as
342 ecosystem engineers : Their associated invertebrate biodiversity under contrasting wave exposures.
343 *Marine Biodiversity*, 44(2), 203-211. <https://doi.org/10.1007/s12526-014-0201-z>

344 Bandara, N., Zeng, H. & Wu, J. (2013). Marine mussel adhesion: biochemistry, mechanisms, and
345 biomimetics. *Journal of Adhesion Science and Technology* 27, 2139–2162.
346 <https://doi.org/10.1080/01694243.2012.697703>

347 Belivermiş, M., Swarzenski, P. W., Oberhänsli, F., Melvin, S. D., & Metian, M. (2020). Effects of
348 variable deoxygenation on trace element bioaccumulation and resulting metabolome profiles in the
349 blue mussel (*Mytilus edulis*). *Chemosphere*, 250, 126314.
350 <https://doi.org/10.1016/j.chemosphere.2020.126314>

351 Bonnefille, B., Gomez, E., Alali, M., Rosain, D., Fenet, H., & Courant, F. (2018). Metabolomics
352 assessment of the effects of diclofenac exposure on *Mytilus galloprovincialis* : Potential effects on
353 osmoregulation and reproduction. *Science of The Total Environment*, 613-614, 611-618.
354 <https://doi.org/10.1016/j.scitotenv.2017.09.146>

355 Campillo, J. A., Sevilla, A., González-Fernández, C., Bellas, J., Bernal, C., Cánovas, M., &
356 Albentosa, M. (2019). Metabolomic responses of mussel *Mytilus galloprovincialis* to fluoranthene
357 exposure under different nutritive conditions. *Marine Environmental Research*, 144, 194-202.
358 <https://doi.org/10.1016/j.marenvres.2019.01.012>

359 Cappello, T., Giannetto, A., Parrino, V., Maisano, M., Oliva, S., De Marco, G., Guerriero, G.,
360 Mauceri, A., & Fasulo, S. (2018). Baseline levels of metabolites in different tissues of mussel *Mytilus*
361 *galloprovincialis* (*Bivalvia* : *Mytilidae*). *Comparative Biochemistry and Physiology Part D: Genomics*
362 *and Proteomics*, 26, 32-39. <https://doi.org/10.1016/j.cbd.2018.03.005>

363 Cappello, T., (2020). NMR-Based Metabolomics of Aquatic Organisms. In: *eMagRes*. John Wiley &
364 Sons, Ltd. 81–100. <https://onlinelibrary.wiley.com/doi/abs/10.1002/9780470034590.emrstml604>.

365 Castro-Portuguez, R., Sutphin, G.L., (2020) Kynurenine pathway, NAD(+) synthesis, and
366 mitochondrial function: Targeting tryptophan metabolism to promote longevity and healthspan.
367 *Experimental Gerontology*, 132,110841. <https://doi.org/10.1016/j.exger.2020.110841>

368 Connor, K. M., & Gracey, A. Y. (2011). Circadian cycles are the dominant transcriptional rhythm in
369 the intertidal mussel *Mytilus californianus*. *Proceedings of the National Academy of Sciences*,
370 108(38),16110-16115. <https://doi.org/10.1073/pnas.1111076108>

371 Connor, K. M., & Gracey, A. Y. (2012). High-resolution analysis of metabolic cycles in the intertidal
372 mussel *Mytilus californianus*. *American Journal of Physiology-Regulatory, Integrative and*
373 *Comparative Physiology*, 302(1), R103-R111. <https://doi.org/10.1152/ajpregu.00453.2011>

374 Courant, F., Antignac, J.-P., Dervilly-Pinel, G., & Le Bizec, B. (2014). Basics of mass spectrometry
375 based metabolomics. *PROTEOMICS*. 14(21-22), 2369-2388. <https://doi.org/10.1002/pmic.201400255>

376 Cubero-Leon, E., Minier, C., Rotchell, J. M., & Hill, E. M. (2012). Metabolomic analysis of sex
377 specific metabolites in gonads of the mussel, *Mytilus edulis*. *Comparative Biochemistry and*
378 *Physiology Part D: Genomics and Proteomics*, 7(2), 212-219.
379 <https://doi.org/10.1016/j.cbd.2012.03.002>

380 Dumas, T., Boccard, J., Gomez, E., Fenet, H. & Courant, F. (2020a). Multifactorial Analysis of
381 Environmental Metabolomic Data in Ecotoxicology: Wild Marine Mussel Exposed to WWTP
382 Effluent as a Case Study. *Metabolites*, 10, <https://doi.org/10.3390/metabo10070269>

383 Dumas, T., Bonnefille, B., Gomez, E., Boccard, J., Castro, N.A., Fenet, H. & Courant, F. (2020b).
384 Metabolomics approach reveals disruption of metabolic pathways in the marine bivalve *Mytilus*
385 *galloprovincialis* exposed to a WWTP effluent extract. *Science of The Total Environment*, 712,
386 136551. <https://doi.org/10.1016/j.scitotenv.2020.136551>

387 Dumas, T., Courant, F., Almunia, C., Boccard, J., Rosain, D., Duporté, G., Armengaud, J., Fenet, H.,
388 & Gomez, E. (2022). An integrated metabolomics and proteogenomics approach reveals molecular
389 alterations following carbamazepine exposure in the male mussel *Mytilus galloprovincialis*.
390 *Chemosphere*, 286, 131793. <https://doi.org/10.1016/j.chemosphere.2021.131793>

391 Dumas, T., Courant, F., Fenet, H., Gomez, E. (2022). Environmental Metabolomics Promises and
392 Achievements in the Field of Aquatic Ecotoxicology: Viewed through the Pharmaceutical Lens.
393 *Metabolites* 12, <https://doi.org/10.3390/metabo12020186>

394 Faggio, C., Tsarpali, V., & Dailianis, S. (2018). Mussel digestive gland as a model tissue for assessing
395 xenobiotics : An overview. *Science of The Total Environment*, 636, 220-229.
396 <https://doi.org/10.1016/j.scitotenv.2018.04.264>

397 Gracey, A. Y., & Connor, K. (2016). Transcriptional and metabolomic characterization of
398 spontaneous metabolic cycles in *Mytilus californianus* under subtidal conditions. *Marine Genomics*,
399 30, 35-41. <https://doi.org/10.1016/j.margen.2016.07.004>

400 Jordan, J., Zare, A., Jackson, L.J., Habibi, H.R. & Weljie, A.M. (2012). Environmental Contaminant
401 Mixtures at Ambient Concentrations Invoke a Metabolic Stress Response in Goldfish Not Predicted
402 from Exposure to Individual Compounds Alone. *Journal of Proteome Research* 11, 1133–1143.
403 <https://doi.org/10.1021/pr200840b>

404 Keskinbalta, M. A., & Çelik, M. Y. (2020). Proximate Composition of Freshwater Mussels (*Unio*
405 *Pictorum*, Linnaeus 1758) in Karasustream, Sinop. *Turkish Journal of Agriculture - Food Science and*
406 *Technology*, 8(9), 1948-1951. <https://doi.org/10.24925/turjaf.v8i9.1948-1951.3584>

407 Kidd, P. M. (2005). GlyceroPhosphoCholine (GPC), Mind-Body Nutrient for Active Living And
408 Healthy Aging. 21.

409 Lin, C. Y., Viant, M. R., & Tjeerdema, R. S. (2006). Metabolomics : Methodologies and applications
410 in the environmental sciences. *Journal of Pesticide Science*, 31(3), 245-251.
411 <https://doi.org/10.1584/jpestics.31.245>

412 Liu, X., Sun, H., Wang, Y., Ma, M., & Zhang, Y. (2014). Gender-specific metabolic responses in
413 hepatopancreas of mussel *Mytilus galloprovincialis* challenged by *Vibrio harveyi*. *Fish & Shellfish*
414 *Immunology*, 40(2), 407-413. <https://doi.org/10.1016/j.fsi.2014.08.002>

415 Lockwood, B. L., Connor, K. M., & Gracey, A. Y. (2015). The environmentally tuned transcriptomes
416 of *Mytilus* mussels. *Journal of Experimental Biology*, 218(12). 1822-1833.
417 <https://doi.org/10.1242/jeb.118190>

418 López-García, E., Postigo, C., & López de Alda, M. (2019). Psychoactive substances in mussels :
419 Analysis and occurrence assessment. *Marine Pollution Bulletin*, 146, 985-992.
420 <https://doi.org/10.1016/j.marpolbul.2019.07.042>

421 Martínez-Pita, I., Sánchez-Lazo, C., Ruíz-Jarabo, I., Herrera, M., & Mancera, J. M. (2012).
422 Biochemical composition, lipid classes, fatty acids and sexual hormones in the mussel *Mytilus*

423 galloprovincialis from cultivated populations in south Spain. *Aquaculture*, 358-359, 274-283.
424 <https://doi.org/10.1016/j.aquaculture.2012.06.003>

425 Moreno-González, R., Rodríguez-Mozaz, S., Huerta, B., Barceló, D., & León, V. M. (2016). Do
426 pharmaceuticals bioaccumulate in marine molluscs and fish from a coastal lagoon? *Environmental*
427 *Research*, 146, 282-298. <https://doi.org/10.1016/j.envres.2016.01.001>

428 Pulliainen, K., Nevalainen, H., Väkeväinen, H., Jutila, K., & Gummer, C. L. (2010). An analytical
429 method for the determination of betaine (trimethylglycine) from hair. *International Journal of*
430 *Cosmetic Science*, 32(2), 135-138. <https://doi.org/10.1111/j.1468-2494.2009.00554.x>

431 Ramirez, G., Gomez, E., Dumas, T., Rosain, D., Mathieu, O., Fenet, H., & Courant, F. (2022). Early
432 Biological Modulations Resulting from 1-Week Venlafaxine Exposure of Marine Mussels *Mytilus*
433 *galloprovincialis* Determined by a Metabolomic Approach. *Metabolites* 12.
434 <https://doi.org/10.3390/metabo12030197>

435 Rochfort, S. J., Ezernieks, V., Maher, A. D., Ingram, B. A., & Olsen, L. (2013). Mussel
436 metabolomics—Species discrimination and provenance determination. *Food Research International*,
437 54(1), 1302-1312. <https://doi.org/10.1016/j.foodres.2013.03.004>

438 Serra-Compte, A., Álvarez-Muñoz, D., Solé, M., Cáceres, N., Barceló, D., & Rodríguez-Mozaz, S.
439 (2019). Comprehensive study of sulfamethoxazole effects in marine mussels : Bioconcentration,
440 enzymatic activities and metabolomics. *Environmental Research*, 173, 12-22.
441 <https://doi.org/10.1016/j.envres.2019.03.021>

442 Song, Q., Chen, H., Li, Y., Zhou, H., Han, Q. & Diao, X. (2016). Toxicological effects of
443 benzo(a)pyrene, {DDT} and their mixture on the green mussel *Perna viridis* revealed by proteomic
444 and metabolomic approaches. *Chemosphere*, 144, 214–224.
445 <http://dx.doi.org/10.1016/j.chemosphere.2015.08.029>

446 Sumner, L. W., Amberg, A., Barrett, D., Beale, M. H., Beger, R., Daykin, C. A., Fan, T. W.-M.,
447 Fiehn, O., Goodacre, R., Griffin, J. L., Hankemeier, T., Hardy, N., Harnly, J., Higashi, R., Kopka, J.,
448 Lane, A. N., Lindon, J. C., Marriott, P., Nicholls, A. W., ... Viant, M. R. (2007). Proposed minimum
449 reporting standards for chemical analysis : Chemical Analysis Working Group (CAWG)
450 Metabolomics Standards Initiative (MSI). *Metabolomics*, 3(3), 211-221.
451 <https://doi.org/10.1007/s11306-007-0082-2>

452 Tomanek, L., & Zuzow, M. J. (2010). The proteomic response of the mussel congeners *Mytilus*
453 *galloprovincialis* and *M. trossulus* to acute heat stress : Implications for thermal tolerance limits and
454 metabolic costs of thermal stress. *Journal of Experimental Biology*, 213(20), 3559-3574.
455 <https://doi.org/10.1242/jeb.041228>

456 Utermann, C., Parrot, D., Breusing, C., Stuckas, H., Staufenberger, T., Blümel, M., Labes, A., &
457 Tasdemir, D. (2018). Combined genotyping, microbial diversity and metabolite profiling studies on
458 farmed *Mytilus* spp. From Kiel Fjord. *Scientific Reports*, 8(1), 7983. <https://doi.org/10.1038/s41598-018-26177-y>

460 Vuckovic, D. (2020). Chapter 4 - Sample preparation in global metabolomics of biological fluids and
461 tissues. In: Issaq HJ, Veenstra TD, editors. *Proteomic and Metabolomic Approaches to Biomarker*
462 *Discovery* (Second Edition). Second Edition. Boston: Academic Press. 53–83.
463 <https://www.sciencedirect.com/science/article/pii/B9780128186077000049>.

464 Yang C, Du X, Hao R, et al (2019) Effect of vitamin D3 on immunity and antioxidant capacity of
465 pearl oyster *Pinctada fucata martensii* after transplantation: Insights from LC-MS-

466 based metabolomics analysis. *Fish Shellfish Immunol* 94:271–279.
467 <https://doi.org/10.1016/j.fsi.2019.09.017>

468 Zhang J, Xiong X, Deng Y, et al (2021) Integrated application of transcriptomics and metabolomics
469 provides insights into the larval metamorphosis of pearl oyster (*Pinctada fucata martensii*).
470 *Aquaculture* 532:736067. <https://doi.org/10.1016/j.aquaculture.2020.736067>

471 Zhang, L., Sun, W., Zhang, Z., Chen, H., Jia, X., & Cai, W. (2017). Gender-specific metabolic
472 responses in gonad of mussel *Perna viridis* to triazophos. *Marine Pollution Bulletin*, 123(1-2), 39-46.
473 <https://doi.org/10.1016/j.marpolbul.2017.09.032>

474
475

476 **Statements & declarations**

477 **Acknowledgements & funding:** This research was funded by SANOFI France and the French Agence
478 Nationale de la Recherche (IMAP ANR-16-CE34-0006-01). The authors thank the Platform Of Non-
479 Target Environmental Metabolomics (PONTEM) of the Montpellier Alliance for Metabolomics and
480 Metabolism Analysis (MAMMA) consortium facilities.

481 .

482

483 **Competing Interests:** The authors have no relevant financial or non-financial interests to disclose.

484

485 **Author contributions:** Lea James: investigation, formal analysis and writing. Elena Gomez:
486 supervision and review. Gaëlle Ramirez : investigation and review. Thibaut Dumas : investigation and
487 review. Frédérique Courant: conceptualization, methodology, supervision and review.

488

489 **Ethics declarations**

490 **Ethical approval:** Ethical approval is exempted in accordance with the European Union directive on
491 the protection of animals used for scientific purposes.

492

493 **Consent to participate:** Not applicable.

494

495 **Consent to publish:** All authors agree to publish.

496

497 **Availability of data and materials:** Not applicable.

498